



Measurements and simulations of scrape-off layer flows in the DIII-D Tokamak

M. Groth^{a,c,*}, G.D. Porter^a, J.A. Boedo^b, N.H. Brooks^c, R.C. Isler^d, W.P. West^c, B.D. Bray^c, M.E. Fenstermacher^a, R.J. Groebner^c, A.W. Leonard^c, R.A. Moyer^b, T.D. Rognlien^a, J.G. Watkins^e, J.H. Yu^b

^a Lawrence Livermore National Laboratory, General Atomics, P.O. Box 85608, Livermore, San Diego, CA 92186-5608, USA

^b University of California San Diego, La Jolla, CA 92093, USA

^c General Atomics, P.O. Box 85608, San Diego, CA 92186-5608, USA

^d Oak Ridge National Laboratory, Oak Ridge, TN 37831, USA

^e Sandia National Laboratory, P.O. Box 5800, Albuquerque, NM 87185, USA

ARTICLE INFO

PACS:
52.25.V
52.30
52.40.H
52.65.K

ABSTRACT

Flow velocities of the order 10–20 km/s in the direction of the high-field side divertor have been measured for deuterons and low charge-state carbon ions in the scrape-off layer at the crown of low-density L-mode plasmas, suggesting that these carbon ions at the crown move with the background plasma flow. Simulations with the multi-fluid edge code UEDGE including cross-field drifts due to $\mathbf{E} \times \mathbf{B}$ and $\mathbf{B} \times \nabla B$ yield calculated divertor conditions which are more consistent with the measurements, but flows at the crown that are stagnant or in the opposite direction than observed. The simulations indicate that both the ion temperature gradient force and deuteron frictional drag play a role in determining the flow direction and magnitude of low charge-state carbon ions. The effect of the assumed radial transport model, toroidal core rotation, and neutral pumping at the divertor plates on the flow at the crown is investigated.

© 2009 Elsevier B.V. All rights reserved.

1. Introduction

Impurity and deuteron flows in the scrape-off layer (SOL) of Tokamaks play a critical role in the long-range migration of eroded materials from the main chamber and divertor surfaces to their final deposition locations [1]. In Tokamaks with carbon-based plasma-facing components (PFC), these flows may transport carbon sputtered off the main chamber wall to the divertor chamber, and thus provide a means of co-deposition of hydrogenic species at the divertor walls in regions shadowed from the plasma. Tritium retention is a serious concern in future, long-pulse fusion devices, such as ITER, where the tritium inventory is restricted [2].

This paper describes measurements of low charge-state carbon ion and deuteron flows at the crown of low-density, low-confinement (L-mode) plasmas in DIII-D. L-mode confinement is used as the simplest plasma condition to avoid SOL perturbations due to edge-localized modes (ELMs) and to permit reciprocating Langmuir probe measurements. The measured deuteron flow is consistent with experimental results from other Tokamaks (see Ref. [3] and references therein) showing near-sonic flow velocities at the crown in configurations with the ion $\mathbf{B} \times \nabla B$ drift toward the divertor X-point (Fig. 3 of [2]). Here, the term ‘crown’ is used to denote the region vertically opposite the divertor X-point. These studies

also report on new measurements using passive Doppler spectroscopy [4] and two-dimensional (2D) imaging [5] at the crown to infer the ion velocities of low charge-state carbon ions at the same poloidal location as the deuteron flow. The experimental data is compared to predictions with the 2D multi-fluid code UEDGE [6], and variations of the transport model and boundary conditions were performed within the code to investigate their effect on the calculated flow-fields.

2. Measurements of SOL flows in the crown of DIII-D L-mode plasmas

2.1. Experimental setup

To enable measurements of low charge-state carbon and deuteron flows at the crown of the plasma in DIII-D, discharges in upper single-null configurations were employed. In these studies, the ion $\mathbf{B} \times \nabla B$ drift was toward the divertor X-point. The core plasma density was low for DIII-D: $\langle n \rangle_{\text{vol}} \sim 2.5 \times 10^{19} \text{ m}^{-3}$ or $\langle n \rangle_{\text{vol}}/n_{\text{CW}} \sim 0.25$. Other discharge parameters include plasma current, I_p , of 1.1 MA, toroidal field, B_T , of 2.0 T, safety factor at the 95% flux surface, q_{95} , of 4.5, and total heating power of 950 kW. Measurements of the upstream separatrix conditions with Thomson scattering and reciprocating Langmuir probes indicate that the SOL is weakly collisional for the electrons: $n_{e,\text{up}} \sim 7 \times 10^{18} \text{ m}^{-3}$, $T_{e,\text{up}} \sim 50 \text{ eV}$, implying a collisionality, ν_e^* , of approximately 7. At the separatrix the ions are significantly hotter and therefore less

* Corresponding author. Address: General Atomics, P.O. Box 85608, San Diego, CA 92186-5608, USA.

E-mail address: groth@fusion.gat.com (M. Groth).

collisional than the electrons: $T_{i,C6+}$ from charge-exchange spectroscopy (CER) is about 150 eV yielding v_i about 0.7. The SOL is therefore expected to be in a sheath-limited regime with the strike points well attached to the target plates. Imaging of carbon emission from the divertor indicated, however, that the strike point at the low-field side (LFS) is attached to the plate, while the high-field side (HFS) divertor appears detached. In the core the toroidal rotation of the C^{6+} ions measured with CER is in the direction of the plasma current at 5–8 km/s at the separatrix and 12–15 km/s at normalized poloidal flux $\Psi_N \sim 0.85$. These plasma conditions were held constant for 3.5 s and methane was injected halfway through the discharge to enhance the carbon emission at the crown for diagnostic purposes. Methane, injected into the lower pumping plenum at LFS, was incident on the crown of the plasma in a toroidally symmetric fashion at a near-constant rate of $1 \text{ Pa/m}^3 \text{ s}$ (8 Torr l/s) for 1.5 s. The injection resulted in a $\sim 20\%$ increase in $\langle n \rangle_{\text{vol}}$ and the SOL radiated power.

2.2. Flow measurements at the crown

Single- and double-charged carbon ions were measured at the crown to flow at velocities of 5–15 km/s parallel to \mathbf{B} in the direction of the HFS divertor (Fig. 1). While the C^{1+} data does not show a strong radial dependence, C^{2+} ions flow at significantly higher velocities nearer to the separatrix. The flow speeds were deduced from the Doppler-shifts of the CII doublet (2P–2S) at 658 nm and the CIII triplet (3P–3S) at 465 nm [4]. These spectroscopic data were taken with a high-resolution spectrometer along two, quasi-tangential view chords (Fig. 2), and referenced against the unshifted profiles measured along vertically (perpendicular) viewing chords. The dependence of the magnetic splitting on the field strength was used to localize the emission observed along the tangential views.

Imaging of the emission from successive dissociation and ionization stages of the methane breakup during the injection into the crown showed the emission plumes being progressively shifted poloidally toward the HFS divertor. Using the measured 2D emission profiles of CI and CII (Fig. 2) and the local SOL plasma

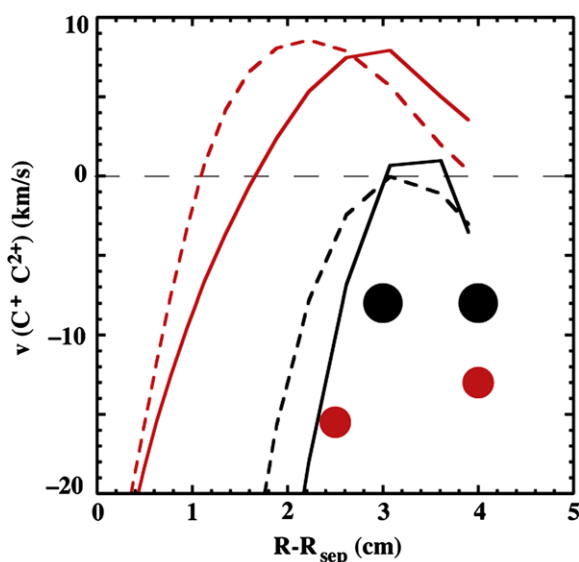


Fig. 1. Comparison of the measured (solid symbols) and UEDGE-simulated (solid lines) ion velocities of C^{1+} (black) and C^{2+} (red) as a function of distance from the separatrix measured at the LFS midplane, $R - R_{\text{sep}}$. Negative velocities denote flow toward the HFS divertor. Cases without cross-field drifts are indicated by solid lines and with drifts by dashed lines. (For interpretation of the references to color in this figure legend, the reader is referred to the web version of this article.)

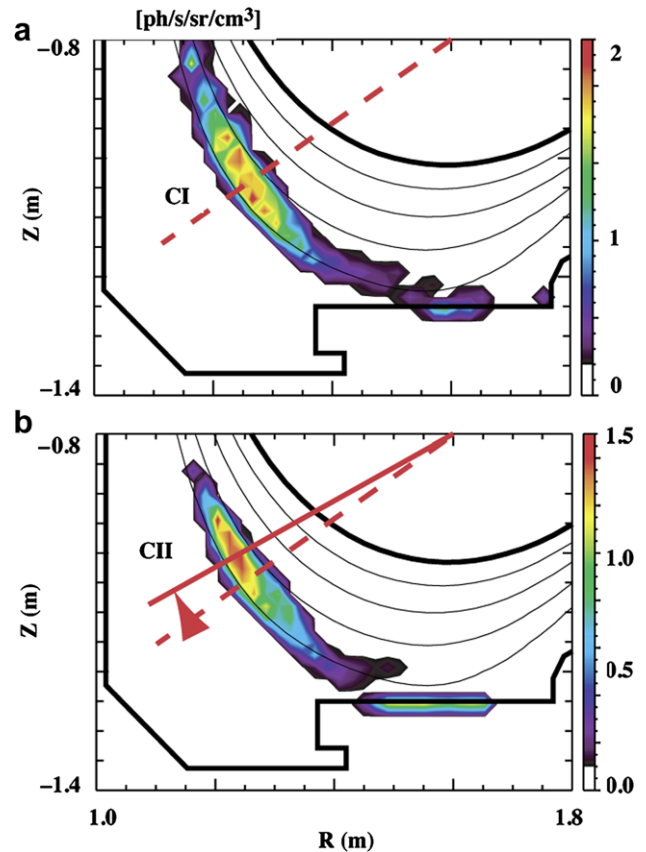


Fig. 2. 2D intensity distributions of: (a) CI (910 nm), and (b) CII (515 nm) emission in the crown during CD_4 injection. The red lines indicate the poloidal shift of the peak CII emission against the CI emission.

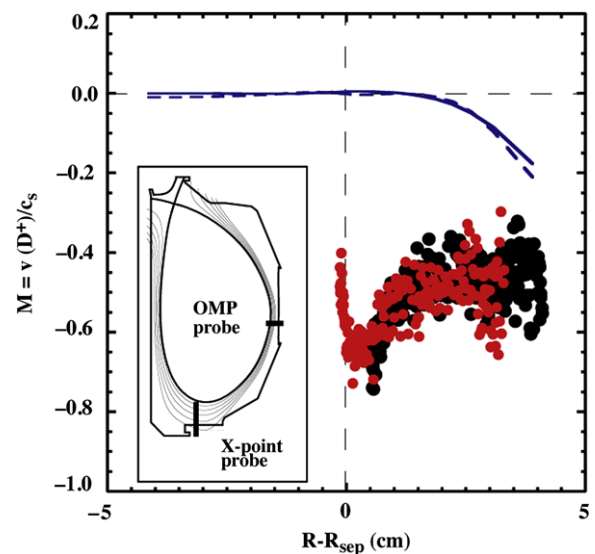


Fig. 3. Comparison of measured (solid symbols) and UEDGE-simulated (solid line) Mach profiles at the crown of the plasma as a function of $R - R_{\text{sep}}$. Two RCP measurements are shown before (black) and during (red) CD_4 injection. The case without drifts is indicated by a blue solid line and with the drifts by a blue dashed line. The insert shows the magnetic geometry as calculated by EFIT [7] and the poloidal location of the RCP. (Data courtesy of J.A. Boedo [10]). (For interpretation of the references to color in this figure legend, the reader is referred to the web version of this article.)

conditions, a poloidal velocity of single ionized carbon of 200–300 m/s can be inferred (Eq. (1) from [5]). The direction and magnitude of the inferred poloidal C^{1+} flow, along with the pitch angles of the total magnetic field determined by EFIT equilibrium reconstruction [7] are consistent with the purely parallel- \mathbf{B} motion measured by Doppler spectroscopy. However, the estimated $\mathbf{E} \times \mathbf{B}$ driven flow is of the same magnitude as the poloidal component of the parallel flow, but in the opposite direction: $\mathbf{E}_{r,SOL} \sim 300$ V/m, thus the $\mathbf{E} \times \mathbf{B}$ poloidal drift velocity ~ 150 m/s [8].

Further evidence of the transport of carbon ions from the crown toward the HFS divertor, rather than toward the LFS divertor, comes from images of the CII (515 nm) and CIII (465 nm) emission from the HFS and LFS midplane regions with tangentially viewing cameras. In the HFS midplane SOL the emission at both wavelengths increased roughly fivefold during methane injection, while only a 10–15% increase was observed at the LFS midplane.

Measurements with a reciprocating, multi-tipped Langmuir probe [9] at the plasma crown show that in the deuterons flow toward the HFS divertor with a velocity parallel to \mathbf{B} of approximately one-half of the local sound speed (Fig. 3, [10]). Referenced to the core plasma current, the SOL deuteron flow is in the same toroidal direction. Using the measured electron temperatures from the probe and assuming $T_e = T_i$, the absolute deuteron speed varies from 35 km/s at the separatrix to 15 km/s in the far SOL. As shown by the two data sets in Fig. 3, the injection of methane did not affect the measurement of the deuteron flow, likely because methane was puffed downstream from the Mach probe.

The measured carbon velocities are consistent with collisional entrainment of the carbon ions in the background deuteron flow, although electrostatic coupling at these densities seems to be marginal for single-charged carbon ions. For the present SOL plasma conditions at the crown, the Spitzer stopping time, τ_s , for collisional drag of D^+ on C^+ [11] is of the order 50 μ s, only one-half of the electron impact ionization time, τ_{ioniz} , for C^+ to C^{2+} . While this is true for low charge-state carbon ions, higher charge-state carbon ions are expected to couple more efficiently to the deuteron flow, as τ_s is proportional to $1/Z^2$, where Z is the charge-state.

3. SOL flow modeling with the UEDGE code

Using the experimental results described in section II, SOL flows have been studied using the 2D multi-fluid edge code UEDGE [6], including the effect of cross-field drifts due to $\mathbf{E} \times \mathbf{B}$ and $\mathbf{B} \times \nabla \mathbf{B}$ [12]. Plasma transport in the \mathbf{B} direction was modeled using the Bragiinski equations, including kinetic corrections, and in the radial direction by assuming a purely diffusive model with radially varying transport coefficients set to match the measured upstream profiles of n_e , T_e , and T_i . Deuterons striking the plates are recycled as neutrals with 100% efficiency, whereas deuterium neutrals striking the plates, the grid boundary facing the private flux region (PFR), and the outermost grid boundary in the main SOL are recycled with 99% efficiency. Carbon released by physical and chemical sputtering at the plates and by chemical sputtering at the walls is injected using published rates [13] into the computational domain as neutral atoms. Its transport and ionization are modeled using a force balance equation in the parallel- \mathbf{B} direction, and diffusion in the radial direction with the same transport coefficients as for the deuterons, and collisional ionization and recombination rates from ADAS [14].

Inclusion of the $\mathbf{E} \times \mathbf{B}$ and $\mathbf{B} \times \nabla \mathbf{B}$ drift terms in the UEDGE fluid equation did neither significantly change the direction and magnitude of the deuteron and C^{2+} ion velocities at the crown, nor improve the agreement with measured flows. It did, however, produce solutions of the divertor plasma that are in better agree-

ment with the measurements. At the crown the calculated deuteron Mach number, $M_{\parallel}^{D^+}$, is zero near the separatrix ($R - R_{sep} < 2$ cm), while its magnitude increases to 0.2 in the direction of HFS divertor in the far SOL ($R - R_{sep} > 2$ cm) (Fig. 3). The parallel- \mathbf{B} velocities of C^{2+} at the crown in the far SOL are opposite the experimental observation; they are of the order 10 km/s in the direction of the LFS divertor (Fig. 1).

The UEDGE simulations indicate that parallel- \mathbf{B} deuteron flow is driven by the pressure gradient between the divertor X-point and the crown produced by recycling in the divertor, $\mathbf{E} \times \mathbf{B}$ driven flow in the PFR, and ion $\mathbf{B} \times \nabla \mathbf{B}$ drifts at the crown and the divertor X-point when the cross-field drifts are included. This flow pattern is offset by radial fluxes across the separatrix, predominately occurring at the LFS midplane. Poloidally, $\mathbf{E} \times \mathbf{B}$ driven flow can be of equal magnitude to the poloidal projection of the parallel flow, or even dominate the flow pattern. Because of the radial electric field being negative in SOL near the separatrix and positive in the far SOL, poloidal $\mathbf{E} \times \mathbf{B}$ driven flow at the crown is toward the HFS divertor in the former region, and toward the LFS divertor in the latter region.

UEDGE indicates that the parallel force balance for C^{2+} is dominated by ion temperature gradient, ∇T_i , force, extending from the high-field X-point region to the crown, and exceeding the frictional force by a factor of 2 at the crown. The simulated ion temperature is high at the LFS midplane region and falls off toward both X-point regions. Poloidally, the flow of low charge-state carbon ions is dominated by the parallel flow components; \mathbf{E}_r in the far SOL (calculated ~ 100 V/m) is too small to play a role. On the other hand, the poloidal flow of higher charge-state carbon ions, carrying the bulk of the total carbon, is determined by both the parallel- \mathbf{B} and $\mathbf{E} \times \mathbf{B}$ components. For $0 < R - R_{sep} < 0.5$ cm, the poloidal C^{4+} flux is governed by $\mathbf{E} \times \mathbf{B}$ drifts in the direction of the HFS divertor, and for $R - R_{sep} > 0.5$ cm the poloidal flow is determined by the parallel- \mathbf{B} component pointing toward the LFS divertor.

Varying the particle and thermal diffusivities poloidally as a function of $1/B_r^n$, where $n = 0, 1, 2, 3$, the magnitude of $M_{\parallel}^{D^+}$ of the deuterons in the far SOL at the crown increases from 0.05 to 0.1 near the separatrix, while the parallel velocity of C^{2+} reverses to flow at approximately 10 km/s toward the HFS divertor. Moving from a weak to a strong ballooning-type transport model ($n = 0 \rightarrow 3$), the ratio of the radial fluxes across the separatrix at the HFS with respect to the LFS midplane is reduced by a factor of 200. It results in a significant reduction of the plasma pressure in the HFS SOL, which produces flow over the crown. These observations are qualitatively consistent with Ref. [15]. The C^{2+} ions flow toward the HFS divertor resulting from a decrease of the parallel ion temperature gradient due to a higher ion temperature in the far SOL.

4. Summary

Measurements of the low charge-state carbon ion and deuteron velocities at the crown of low-density L-mode plasmas with ion $\nabla \mathbf{B}$ drift toward the divertor X-point show that these plasma species flow at similar, near-sonic magnitude toward the HFS divertor plate. These results are qualitatively consistent with our previous conclusions drawn from the deposition pattern in DIII-D ^{13}C isotope tracer experiments [5]. Inference from the poloidal flow component of C^{1+} ions and measurements of the local plasma conditions suggests, however, that entrainment of low charge-state carbon ions in the background ion flow is weak, while higher charge-state carbon ions are expected to couple more efficiently to the deuterons.

Simulations with the UEDGE code highlight the significance of cross-field drifts and assumptions of the radial transport models:

while solutions from simulations with the $\mathbf{E} \times \mathbf{B}$ and $\mathbf{B} \times \nabla \mathbf{B}$ drift are more consistent with measurements of the local parameters in the divertor, they produce a stagnant background SOL plasma at the crown. The ion temperature gradient force dominates over the frictional force exerted by the deuterons at the crown causing low charge-state carbon ions to flow toward the LFS divertor. Unfortunately, ion temperature measurements in the SOL are scarce and, thus, the effect of their gradients on impurity ion transport can only be assessed numerically. Imposing strong poloidal asymmetries on the radial fluxes by choice of the transport coefficients can force deuterium and low charge-state carbon flow toward the HFS plate at the crown. The predicted profile and magnitude of the deuterium flow still falls short to match experimental data.

Acknowledgment

This work performed under the auspices of the US Department of Energy by Lawrence Livermore National Laboratory under

Contract DE-AC52-07NA27344, DE-FC02-04ER54698, DE-FG02-07ER54917, DE-AC05-00OR22725 and DE-AC04-94AL85000.

References

- [1] G.F. Matthew et al., *J. Nucl. Mater.* 337–339 (2005) 1.
- [2] B. Lipschultz et al., *Nucl. Fus.* 47 (2007) 1189.
- [3] N. Asakura et al., *J. Nucl. Mater.* 363–365 (2007) 41.
- [4] R.C. Isler et al., *Phys. Plasma* 6 (1999) 1837.
- [5] M. Groth et al., *Phys. Plasma* 14 (2007) 056120.
- [6] T.D. Rognlien et al., *J. Nucl. Mater.* 196–198 (1992) 347.
- [7] L.L. Lao et al., *Nucl. Fus.* 25 (1985) 1611.
- [8] P.C. Stangeby, *The Plasma Boundary of Magnetic Fusion Devices*, Institute of Physics Publishing Ltd., Bristol, 2000.
- [9] J.G. Watkins et al., *Rev. Sci. Instrum.* 68 (1997) 373.
- [10] J.A. Boedo et al., *Phys. Plasma*, this issue.
- [11] L. Spitzer, *Physics of Fully Ionized Gases*, 2nd Ed., Wiley, New York, 1962.
- [12] T.D. Rognlien et al., *J. Nucl. Mater.* 266–269 (1999) 654.
- [13] J.W. Davis et al., *J. Nucl. Mater.* 241–243 (1997) 37.
- [14] ADAS Atomic Data and Analysis Structure, ADAS News, The ADAS Project, 1995–2008.
- [15] A. Yu Pigarov et al., *Contrib. Plasma Phys.* 48 (2008) 82.